Remote Sensing of Environment 124 (2012) 394–401

Contents lists available at SciVerse ScienceDirect

Remote Sensing of Environment

journal homepage: www.elsevier.com/locate/rse

Statistical inference for remote sensing-based estimates of net deforestation

Ronald E. McRoberts *, Brian F. Walters

Northern Research Station, U.S. Forest Service, Saint Paul, Minnesota, USA

ARTICLE INFO

Article history:
Received 11 July 2011
Received in revised form 10 May 2012
Accepted 11 May 2012
Available online 20 June 2012

Keywords:
Landsat
Forest inventory
Error matrix
Model-assisted estimator

ABSTRACT

Statistical inference requires expression of an estimate in probabilistic terms, usually in the form of a confidence interval. An approach to constructing confidence intervals for remote sensing-based estimates of net deforestation is illustrated. The approach is based on post-classification methods using two independent forest/non-forest classifications because sufficient numbers of observations of forest/non-forest change were not available for direct classification. Further, the approach uses a model-assisted estimator with information from a traditional error matrix for the forest/non-forest classifications to compensate for bias as the result of classification errors and to estimate variances. Classifications were obtained using a logistic regression model, forest inventory data, and two dates of Landsat imagery, although the approach to inference can be used with multiple classification approaches. For the study area in northeastern Minnesota, USA, overall pixel-level accuracies for the year 2002 and 2007 forest/non-forest classifications were 0.85–0.88, and estimates of proportion net deforestation for the 2002–2007 interval were less in absolute value than 0.015. However, standard errors for the remote sensing-based estimates of net deforestation were on the order of 0.02–0.04, meaning that the estimates were not statistically significantly different from zero. Particular attention is directed to the potentially severe sample size and classification accuracy requirements necessary for estimates of net deforestation to be detected as statistically significantly different from zero.

Published by Elsevier Inc.

1. Introduction

1.1. Background and motivation

Forest ecosystems are among the most biologically rich and genetically diverse terrestrial ecosystems on earth. Of the 38 main classes in Holdridge's (1947, 1967) life zone classification, more than half (19 forest and two woodland formations) are dominated by trees. The World Wildlife Fund (Dinerstein et al., 1995) identified 14 major earth habitat types of which seven are forest types. Depending on definitions, 22–30% of the earth's surface is covered by forests and wooded lands (FAO, 2005; GFW, 2006). Further, these lands provide habitat for 70% of known animal and plant species (Matthews et al., 2000) and contribute almost half the terrestrial net primary biomass production (Groombridge & Jenkins, 2002). Thus, forests provide vital economic, social, and environmental benefits by supplying wood and non-wood forest products, supporting human livelihoods, supplying clean water, and providing habitat for half the species on the planet.

The forestry sector also plays a vital role in the global greenhouse gas (GHG) balance. The approximately 13 million hectares (ha) of forest that are converted to other land uses annually worldwide (FAO, 2005, p. 13) account for as much as 25% of anthropogenic GHG emissions (Achard et al., 2002; Gullison et al., 2007). Conversely, among the five economic sectors identified by the United Nations Framework Convention on Climate Change (UNFCCC) as sources of anthropogenic GHG emissions, only the Land Use, Land Use Change Forestry (LULUCF) sector has the potential for removal of GHG emissions from the atmosphere. The Intergovernmental Panel on Climate Change (IPCC) estimated that this mitigation potential is as great as 50% of the total potential (Nabuurs & Masera, 2007, p. 543).

GHG emission accounting, as a form of carbon accounting, assesses the scale of emissions from the forestry sector relative to other sectors. Two primary approaches to emission accounting are common, the stock difference or inventory approach and the gain-loss or activity approach (Köhl et al., 2009). With the stock-difference approach, annual emissions are estimated as the mean annual difference in carbon stocks between two points in time. For countries with established national forest inventories (NFI), the stock-difference approach is fairly easy to implement. However, for countries without established NFIs, particularly developing tropical countries with remote and inaccessible forests, the inventory approach may be prohibitively expensive, even with external financial and logistical support. For these countries, the gain–loss approach is an alternative; in fact, Giardin (2010) asserts that the gain–loss approach is the most commonly used approach for estimating GHG emissions for national measurement, reporting, and verification (MRV) systems under the auspices of the IPCC. With this approach, the net balance of additions to and removals from a carbon pool is estimated as the product of the rate of

* Corresponding author. Tel.: +1 651 649 5174; fax: +1 651 649 5140.
E-mail address: rmcroberts@fs.fed.us (R.E. McRoberts).

0034-4257/$ – see front matter. Published by Elsevier Inc.
doi:10.1016/j.rse.2012.05.011

land use area change, called activity data, and the responses of carbon stocks for particular land use changes, called emission factors. Giardin (2010) notes that MRV systems typically include ground-based inventories for estimating emission factors and remote sensing-based components for estimating activity data for forest area and forest area change. The GOFC-GOLD Sourcebook (2010, Chapter 2) further emphasizes the role of satellite remote sensing as an important tool for monitoring changes in forest cover. Finally, Köhl et al. (2009) and Watson (2009) assert that good practice requires that uncertainty in estimates of emission factors and activity data should be expressed in the form of 95% confidence intervals.

1.2. Methods review

Two basic premises underlie the use of multi-spectral remotely sensed data for estimation of activity data in the form of land cover change such as deforestation, afforestation, and reforestation: (1) changes in land cover produce changes in radiance values, and (2) changes in radiance caused by land cover change are large compared to changes in radiance changes caused by other factors (Singh, 1989). Thus, the essence of remote sensing-based change detection is "comparing the position of a pixel in spectral space between different points in time" (Kennedy et al., 2009). Further, characterization of the type, extent, and intensity of change depends on understanding the link between the conversion, modification, and condition of land cover and spectral variability (Hayes & Cohen, 2007).

Remote sensing-based change detection methods include two primary categories, trajectory analysis and bi-temporal methods. Trajectory analyses use time series of three or more images to assess not only the type and extent of change but also the progress, trend, or temporal patterns of change over time (Kennedy, et al., 2007). Bi-temporal methods entail the analyses of two images for different dates and can be further separated into two subcategories. The first subcategory, post-classification, entails comparison of two classifications that are constructed separately using remotely sensed data from two dates (Coppin et al., 2004). The second subcategory, direct classification, entails classification of change from ground observations of change and two sets of remotely sensed data that have been merged into a single dataset (Hayes & Cohen, 2007).

For predicting change in categorical variables such as forest/non-forest or classes of forest change, logistic regression models have been used successfully. Fraser et al. (2003, 2005), and Fraser and Latifovic (2005) used logistic regression with two-date change metrics obtained from SPOT and AVHRR data to map deforestation in Quebec, Canada, resulting from multiple causes including insect defoliation, burning, flooding, and harvest. Accuracies were greater than 90% with small omission and commission errors. Wulder et al. (2006) used logistic regression with multi-date Landsat, topographic, and solar radiation variables to detect deforestation in British Columbia, Canada, resulting from the mountain pine beetle. Accuracy was approximately 85%. In summary, logistic regression has been found useful for predicting dichotomous or polychotomous classes of deforestation from a variety of causes in a wide range of geographic regions.

The overwhelming majority of techniques for assessing the accuracy of classifications, including change classifications, regardless of the data or classification method, are based on error or confusion matrices and measures derived from them (Hayes & Sader, 2001; Kennedy et al., 2009; Mas, 1999; Muchoney & Haack, 1994). Card (1982) and Czaplewski and Catts (1992) extended error matrices to inferences for the accuracies of individual class predictions. Of importance, error matrices and their associated indices and accuracies do not constitute inferences in the form of the confidence intervals that are required for activity data such as area of deforestation. For single-date areal estimation, Walsh and Burk (1993) used error matrices to compare the classical and inverse estimators specifically for use with linear regression models, and Van Deusen (1994) used error matrices as the context for investigating sampling schemes to enhance estimates of change obtained from two thematic maps.

1.3. Objectives

The overall objective of the study was to develop an approach to inference in the form of confidence intervals for estimates of net deforestation (Kauppi et al., 2006; Meyfroidt et al., 2010) using a combination of forest inventory and satellite image data. In this context, net deforestation is defined as the net result of removals from and additions to forest cover and is distinguished from deforestation which is simply the loss of forest cover. Although in the context of programs aimed at reducing emissions from deforestation and forest degradation (REDD) only human-induced forest loss is considered deforestation, the focus of this study is simply net change in forest cover, regardless of the cause. The overall objective was addressed using a probability-based (design-based), model-assisted approach to constructing confidence intervals for estimates of net deforestation. When deforestation is a rare event, which is often the case, and when training data are acquired using equal probability sampling designs, the number of observations of forest/non-forest change may be insufficient to support a direct classification approach. Such was the case for this study for which an average of only four plots per year changed from forest to non-forest or vice versa. Therefore, only post-classification approaches were considered. The study was conducted using a logistic regression model with two dates of Landsat Thematic Mapper (TM) imagery and multiple dates of forest inventory data, although the approach to inference is applicable for use with other approaches to classification.

2. Data

The study area was defined by the portion of the row 27, path 27, Landsat scene in northern Minnesota, USA, that was cloud-free for the two image dates, 16 July 2002 and 30 July 2007 (Fig. 1). Spectral data in the form of the normalized difference vegetation index (NDVI) transformation (Rouse et al., 1973) and the three tasseled cap (TC) transformations (brightness, greenness, and wetness) (Crist & Cicone, 1984; Kauth & Thomas, 1976) for each of the two image dates were used.

Ground data were obtained for plots established by the Forest Inventory and Analysis (FIA) program of the U.S. Forest Service which conducts the NFI of the USA. The program has established field plot centers in permanent locations using a sampling design that is regarded as producing an equal probability sample (McRoberts et al., 2005). Each FIA plot consists of four 7.32-m (24-ft) radius circular subplots that are configured as a central subplot and three peripheral subplots with centers located at distances of 36.58 m (120 ft) and azimuths of 0°, 120°, and 240° from the center of the central subplot. In general, centers of forested, partially forested, or previously forested plots are determined using global positioning system (GPS) receivers, whereas centers of non-forested plots are verified using aerial imagery and digitization methods. Each year between 2000 and 2004 approximately 246 plots were measured; the same plots were remeasured at 5-year intervals between 2005 and 2009. Field crews visually estimate the proportion of each subplot that satisfies the FIA definition of forest land: minimum area of 0.4 ha (1.0 ac), minimum crown cover of 10%, minimum crown cover width of 36.6 m (120 ft), and forest land use. Field crews also observe species and measure diameter at-breast-height (dbh) (1.37 m, 4.5 ft) and height for all trees with dbh of at least 12.7 cm (5 in.). Growing stock volumes of individual measured trees are estimated using statistical models, aggregated at subplot-level, expressed as volume per unit area, and considered to be observations without error. Subplot-level proportion forest and volume data were combined

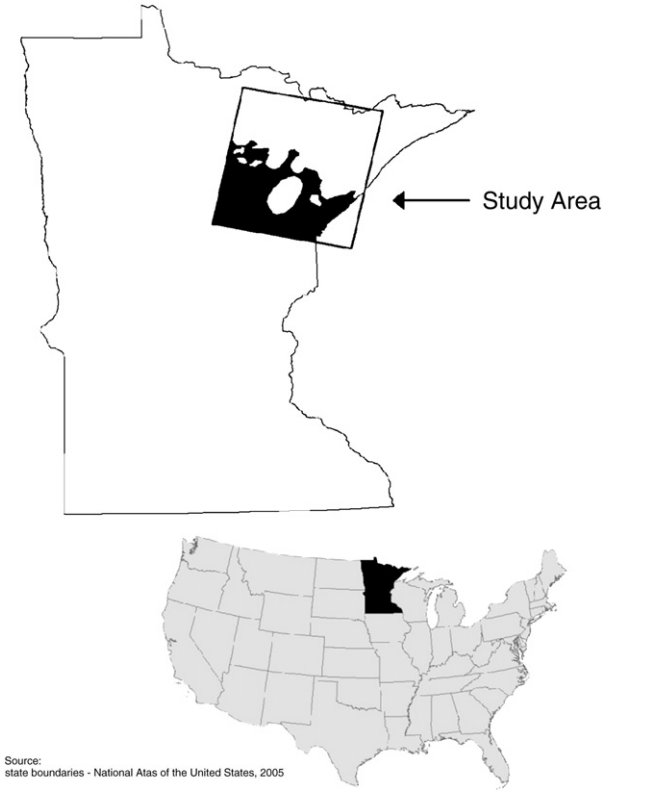

Fig. 1. Study area in northeastern Minnesota, USA (portion of Landsat path 27, row 27 that was cloud free for both image dates).

with the values of the spectral transformations for pixels containing subplot centers.

For construction of training and accuracy assessment datasets, data for only the central subplot of each plot were used for this study to avoid issues related to spatial correlation among observations for subplots of the same plot. For future reference, the term *plot* refers to the central subplot of each FIA plot cluster. Additional details regarding construction of training and accuracy datasets are reported in Section 3.3.

3. Methods

3.1. Logistic regression

The relationship between a dichotomous response variable, Y (assumes values $y=0$ and $y=1$), and continuous independent variables, $\mathbf{X}$, is often expressed in the form,

$$p_i = f(\mathbf{X}_i;\boldsymbol{\beta}),$$

where i indexes population units, p_i is the probability that $y_i=1$, and $\boldsymbol{\beta}$ is a vector of parameters to be estimated (Agresti, 2007). The function, $f(\mathbf{X}_i;\boldsymbol{\beta})$, expresses the statistical expectation of Y in terms of $\mathbf{X}$ and $\boldsymbol{\beta}$ and is often formulated using the logistic function as,

$$p_i = f(\mathbf{X}_i;\boldsymbol{\beta}) = \frac{\exp\left(\sum_{j=1}^{J}\beta_j x_{ij}\right)}{1+\exp\left(\sum_{j=1}^{J}\beta_j x_{ij}\right)}, \quad (1)$$

where $j=1, 2,\ldots, J$ indexes the independent variables, and exp(.) is the exponential function.

3.2. Inference

Probability-based inference, also characterized as design-based inference, is based on three assumptions: (1) population units are selected for the sample using a randomization scheme; (2) the probability of selection for each population unit into the sample is positive and known; and (3) the value of the response variable for each population unit is a fixed value as opposed to a random variable. Properties of probability-based estimators are based on random variation resulting from the probabilities of selection of population units into the sample, thus the characterization of these estimators as probability-based (Hansen et al., 1983).

With probability-based methods, observations and predictions of a categorical response variable are both in the form of discrete classes. For the categorical forest/non-forest variable, Y,

$$y_i = \begin{cases} 0 & \textit{if the non-forest class is observed for the ith population unit} \\ 1 & \textit{if the forest class is observed for the ith population unit} \end{cases} \quad (2a)$$

and

$$\hat{y}_i = \begin{cases} 0 & \textit{if the non-forest class is predicted } (\hat{p}_i<0.5) \textit{ for the ith population unit} \\ 1 & \textit{if the forest class is predicted } (\hat{p}_i\geq 0.5) \textit{ for the ith population unit} \end{cases}, \quad (2b)$$

where $\hat{p}_i$ is the predicted probability of forest from Eq. (1).

An error matrix (Table 1) depicts the numbers or proportions of observations and predictions by class and informs measures of accuracy: *overall accuracy* (OA), which is the proportion of observations correctly classified; *producer's accuracy* (PA), which is the ratio of the number of correct predictions and the total number of observations for a class; and *user's accuracy* (UA), which is the ratio of the number of correct predictions and the total number of predictions for a class (Congalton, 1991).

Error matrices do not directly provide variances for estimates of class areas or proportions and, therefore, do constitute inferences in the form of confidence intervals for parameters of populations depicted by remote sensing-based classifications. Assuming a classification, a probability accuracy assessment sample, and a properly formulated error matrix, construction of a confidence interval requires an unbiased or nearly unbiased estimator of the population parameter of interest and a variance estimator.

For areal assessments, the objective is typically to estimate the total area or proportion of a class of the response variable. Because the estimate of the total area of a class is simply the product of total area which is usually known and the estimate of the class proportion, the focus of this study is estimation of the proportion.

Model-assisted estimators rely on observations for population units selected for the sample and model predictions for population units not selected for the sample. However, because the validity of an inference is still based on the probability sample, the estimator is

Table 1
Error matrix.

		Predicted class		Total	Producer's Accuracy (PA)
		$\frac{0}{(NF)}$	$\frac{1}{(F)}$		
Observed class	0 (NF)	n_{00}	n_{01}	n_{0+}	$\frac{n_{00}}{n_{0+}}$
	1 (F)	n_{10}	n_{11}	n_{1+}	$\frac{n_{11}}{n_{1+}}$
Total		n_{+0}	n_{+1}	n	
User's accuracy (UA)		$\frac{n_{00}}{n_{+0}}$	$\frac{n_{11}}{n_{+1}}$		$OA=\frac{n_{00}+n_{11}}{n}$

characterized as probability-based. A naïve model-assisted estimator of proportion forest, μ_F, is,

$$\hat{\mu}_{F,naive} = \frac{1}{N}\left(\sum_{i=1}^{n} y_i + \sum_{i=n+1}^{N} \hat{y}_i\right), \tag{4}$$

where n is the sample size, N is the population size, and the population has been indexed so that i = 1,2,…,n denotes the sampled population units with observations, y_i, and i = n + 1,n + 2,…,N denotes the non-sampled population units with predictions, $\hat{y}_i$. For equal probability samples, the bias associated with this estimator may be estimated as,

$$\begin{aligned} \hat{Bias}\left(\hat{\mu}_{F,naive}\right) &= \frac{1}{n}\sum_{i=1}^{n}(\hat{y}_i - y_i) \\ &= \frac{n_{01} - n_{10}}{n}, \end{aligned} \tag{5}$$

where n_{01} and n_{10} are obtained from the error matrix (Table 1). The model-assisted estimator (Särndal et al., 1992) for proportion forest, μ_F, is defined as the difference between the naïve estimator and the expectation of its bias estimate which, under the assumptions that N is both large and much larger than n, can be approximated as,

$$\hat{\mu}_F = \frac{1}{N}\sum_{i=1}^{N} \hat{y}_i - \frac{n_{01} - n_{10}}{n}. \tag{6}$$

Under the assumptions that N is both large and much larger than n, that the errors are independent, and that simple random sampling was used, the variance of $\hat{\mu}_F$ can be approximated as,

$$\begin{aligned} \hat{Var}(\hat{\mu}_F) &= \frac{1}{n}\hat{Var}(\hat{y}_i - y_i) \\ &= \frac{1}{n(n-1)}\left\{\sum_{i=1}^{n}(\hat{y}_i - y_i)^2 - \frac{1}{n}\left[\sum_{i=1}^{n}(\hat{y}_i - y_i)\right]^2\right\} \\ &= \frac{1}{n(n-1)}\left[(n_{01} + n_{10}) - \frac{1}{n}(n_{01} - n_{10})^2\right] \\ &= \frac{1}{(n-1)}\left[(1 - OA) - \hat{Bias}\left(\hat{\mu}_{F,naive}\right)^2\right]. \end{aligned} \tag{7}$$

When systematic sampling rather than simple random sampling is used, variances may be overestimated (Särndal et al., 1992). Eqs. (5)–(7) demonstrate that although error matrices do not constitute inferences in the form of the required confidence intervals and do not directly assess bias and precision of population parameters, they do provide much of the information necessary for doing so when using the model-assisted estimator.

For the forest class, an inference in the form of a confidence interval is expressed as,

$$\hat{\mu}_F \pm t_{1-\frac{\alpha}{2}}\sqrt{\hat{Var}(\hat{\mu}_F)}, \tag{8}$$

where $t_{1-\frac{\alpha}{2}}$ refers to the $1-\frac{\alpha}{2}$ percentile of Student's t-distribution. For applications for which either positive or negative estimates of net deforestation are of interest, such as NFIs, $1-\frac{\alpha}{2}$ would be commonly used for constructing confidence intervals and testing hypotheses, whereas for climate change applications for which primary interest may be loss of forest area which corresponds to only negative values of net deforestation, $1-\alpha$ may be appropriate. For this study, $1-\frac{\alpha}{2}$ was used because of interest in any change in forest cover, not just loss of cover. Of considerable importance, this approach to inference using the model-assisted estimator as formulated using Eqs. (4)–(8) can be used with multiple approaches to classification, although it depends on accuracy assessment data obtained for an equal probability sample.

For the post-classification approach to change assessment, the estimator of net deforestation is,

$$\Delta\hat{\mu}_F = \hat{\mu}_F^2 - \hat{\mu}_F^1, \tag{9}$$

where Δ denotes change, μ_F denotes proportion forest, and the superscripts denote times 1 and 2. The estimator of $Var(\Delta\hat{\mu}_F)$ is,

$$\begin{aligned} \hat{Var}(\Delta\hat{\mu}_F) &= \hat{Var}\left(\hat{\mu}_F^2 - \hat{\mu}_F^1\right) \\ &= \hat{Var}\left(\hat{\mu}_F^2\right) - 2\hat{Cov}\left(\hat{\mu}_F^2, \hat{\mu}_F^1\right) + \hat{Var}\left(\hat{\mu}_F^1\right). \end{aligned} \tag{10a}$$

Because $\hat{\mu}_F^1$ and $\hat{\mu}_F^2$ are estimates from single date classifications, $\hat{Var}(\hat{\mu}_F^1)$ and $\hat{Var}(\hat{\mu}_F^2)$ can be calculated using Eq. (7). If the two accuracy assessment datasets are mutually independent, then $Cov(\hat{\mu}_F^2, \hat{\mu}_F^1) = 0$ with the result that,

$$\hat{Var}(\Delta\hat{\mu}_F) = \hat{Var}\left(\hat{\mu}_F^2\right) + \hat{Var}\left(\hat{\mu}_F^1\right). \tag{10b}$$

When the accuracy assessment datasets consist of observations of the same mapping units, albeit at different times, the covariance cannot be assumed to be zero, but it can be estimated as,

$$\hat{Cov}\left(\hat{\mu}_F^2, \hat{\mu}_F^1\right) = \frac{1}{n(n-1)}\sum_{i=1}^{n}\left(\delta_i^1 - \bar{\delta}^1\right)\left(\delta_i^2 - \bar{\delta}^2\right), \tag{11}$$

where $\delta_i^1 = \hat{y}_i^1 - y_i^1$ and $\delta_i^2 = \hat{y}_i^2 - y_i^2$ are classification errors, $\bar{\delta}^1$ and $\bar{\delta}^2$ are corresponding means of errors, and the superscripts again denote times 1 and 2.

3.3. Training and accuracy assessment datasets

Four concerns must be addressed when constructing training and accuracy datasets using the FIA plot data and Landsat imagery. First, observations included in the training and accuracy datasets should be independent; otherwise, accuracy assessments will be optimistic, and the resulting confidence intervals will be too small. For this study, independence is ensured by constructing training and accuracy assessment datasets so that they contain no observations for any of the same plots. Second, the forest and non-forest proportions for the smaller 168.3-m^2 plots may not adequately characterize the proportions for the larger 900-m^2 TM pixels containing the plot centers. The concern is at least partially alleviated by using observations for only completely forested and completely non-forested plots.

Third, FIA field crews classify plots on the basis of land use, not land cover. Thus, plots whose tree cover has been removed are still classified as forest if trees are expected to regenerate and if the land use is expected to remain forest. A possible result is that a plot classified by a field crew as forest with respect to land use may, in fact, have no forest cover due to recent harvest or other causes. If so, a forest plot observation may be associated with spectral values characteristic of non-forest. Alternatively, a non-forest observation may be arbitrarily assigned to the plot, but it may then be associated with spectral values associated with forest if the harvest condition on the smaller plot did not extend to the entire larger pixel. To alleviate this concern, observations for plots classified by field crews as having forest land use but with no volume are omitted from the remote sensing analyses.

Fourth, the likelihood that the forest/non-forest status of a plot changes between the plot measurement and image dates increases as the elapsed time between the two dates increases. If such a change occurs, a forest plot observation may again be associated with spectral values characteristic of non-forest, and vice versa. To alleviate this concern, the fact that each plot was measured on two occasions

can be exploited. For example, the plots that were measured in 2000 are the same plots that were measured in 2005. Therefore, plots that had forest or non-forest cover in both 2000 and 2005 are relatively certain to also have had forest or non-forest cover, respectively, in 2002, the image date. The concern was alleviated by restricting the remote sensing analyses to plots whose forest and non-forest observations did not change between 2000 and 2005, 2001 and 2006, 2003 and 2008, and 2005 and 2009. The effect of the latter action is that forest and non-forest observations for plots included in the analyses are same for both measurement dates. The situation for plots measured in 2002 and 2007 is addressed below.

Subject to alleviation of the four concerns a training dataset and two accuracy assessment datasets were constructed for each image date. First, the data for plots measured in 2000 and again in 2005 and the data for plots measured in 2001 and again in 2006 were pooled and randomly divided into two independent datasets, one designated as the 2002 training dataset (T_{2002}) and the other designated as the first 2002 accuracy assessment dataset ($A_{2002\text{-}1}$). Similarly, the data for plots measured in 2003 and again in 2008 and data for plots measured in 2004 and again in 2009 were pooled and randomly divided into two independent datasets, one designated as the 2007 training dataset (T_{2007}) and the other designated as the first 2007 accuracy assessment dataset ($A_{2007\text{-}1}$). Of importance, these four datasets are mutually independent because observations for no plots, at either measurement date, are included in more than one dataset. As a result, $\hat{Var}(\Delta\hat{\mu}_F)$ may be calculated using Eq. (10b).

A second accuracy assessment dataset was constructed for each image date. Subject to alleviation of the first three concerns, the 2002 plot observations were designated as the second 2002 accuracy assessment dataset ($A_{2002\text{-}2}$) and the 2007 plot observations were designated as the second 2007 accuracy assessment dataset ($A_{2007\text{-}2}$). Three features of these two datasets are important. First, no accommodation was made for the fourth concern for these datasets. Because the exact plot measurement dates were not available, no determination could be made as to whether a plot was measured before or after the image date. As a result, even if the forest/non-forest covers for a plot were the same for the 2002 and 2007 plot measurement dates, there is no assurance that they were the same for the two image dates. However, because the plot measurement and image dates were in the same year, the probabilities of change in cover between the plot measurement and image dates were small. Second, observations for the two datasets are independent of observations for the two training datasets. Third, however, observations for the two datasets are not independent because the same plots that were measured in 2002 were also measured in 2007. Thus, the plot observations for these two accuracy assessment datasets are likely to be positively correlated which results in $\hat{Cov}(\hat{\mu}_F^2, \hat{\mu}_F^1) > 0$ so that $\hat{Var}(\Delta\hat{\mu}_F)$ must be calculated using Eq. (10a).

The net effect of alleviating the concerns was to reduce the number of plots whose observations were used for the analyses from an average of 246 to an average of 196 per year, a decrease of approximately 20%. For inferential purposes, the plots whose data were omitted from the analyses to accommodate the concerns were considered to be a random selection from the original FIA sample.

3.4. Analyses

3.4.1. Sample size determination

One result of the simple relationship between $\hat{Var}(\hat{\mu}_F)$, OA, and $\hat{Bias}\left(\hat{\mu}_{F,naive}\right)$ as expressed by Eq.(7) is that accuracy assessment sample sizes, n, necessary for net deforestation of given magnitudes to be detected as statistically significantly different from zero can be readily calculated. For two classifications with the same OA and the same $\hat{Bias}\left(\hat{\mu}_{F,naive}\right)$ obtained from accuracy assessment datasets whose observations are independent, net deforestation, d, may be equated to the product of the standard error and the standard Gaussian quantile, Z, for the desired significance level to obtain,

$$\begin{aligned} d &= Z_{1-\alpha}\cdot SE\left(\hat{\Delta\mu}_F\right) \\ &= Z_{1-\alpha}\cdot\sqrt{\hat{Var}(\hat{\mu}_F^2)+\hat{Var}(\hat{\mu}_F^1)} \\ &= Z_{1-\alpha}\cdot\sqrt{2\left[\frac{(1-OA)-\hat{Bias}\left(\hat{\mu}_{F,naive}\right)^2}{n-1}\right]} \end{aligned}$$

from which,

$$n = 1+\frac{2\cdot Z_{1-\alpha}^2\cdot\left[(1-OA)-\hat{Bias}\left(\hat{\mu}_{F,naive}\right)^2\right]}{d^2}, \tag{12a}$$

where α denotes the statistical significance desired; $\alpha = 0.05$ is often selected. However, this value of n yields probability of only 0.50 that net deforestation of d will be detected as statistically significantly different from zero at the α level. To increase this probability, commonly characterized as statistical power, Eq. (12a) is modified to,

$$n = 1+\frac{2\cdot\left(Z_{1-\alpha}+Z_{1-\beta}\right)^2\cdot\left[(1-OA)-\hat{Bias}\left(\hat{\mu}_{F,naive}\right)^2\right]}{d^2}, \tag{12b}$$

where 1-β denotes the probability that net deforestation, d, will be detected as statistically significantly different from zero; $\beta = 0.20$ is often selected. A graph of the relationship between n and d for selected values of OA and $\hat{Bias}\left(\hat{\mu}_{F,naive}\right)$ using $1\text{-}\alpha = 0.95$ and $1\text{-}\beta = 0.80$ was constructed.

3.4.2. Accuracy assessment

The logistic regression model was fit to the T_{2002} and T_{2007} datasets, and the model parameters were estimated. For each dataset, a lack of fit assessment was conducted using three steps: (i) the pairs $(y_i, \hat{p}_i)$ were ordered with respect to $\hat{p}_i$ obtained from Eq. (1), (ii) the ordered pairs were aggregated into groups of size 15, and (iii) the group means of the observations, y_i, were graphed versus the group means of the estimates, $\hat{p}_i$(Hosmer & Lemeshow, 1989).

For the 2002 classification based on model parameters estimated from the T_{2002} dataset, error matrices were constructed using both the $A_{2002\text{-}1}$ and $A_{2002\text{-}2}$ accuracy assessment datasets. Similarly, two error matrices were constructed for the 2007 classification, one each for the $A_{2007\text{-}1}$ and $A_{2007\text{-}2}$ accuracy assessment datasets. For each of the four error matrices, PA, UA, and OA were calculated.

3.4.3. Estimation of net deforestation

The logistic regression model with parameters estimated from the T_{2002} training dataset was used with the 2002 image data to construct a forest/non-forest classification for the study area (Fig. 1), and $\hat{\mu}_{F,naive}^{2002}$ was calculated using Eq. (4). Using information from the two error matrices based on the $A_{2002\text{-}1}$ and $A_{2002\text{-}2}$ accuracy assessment datasets, two values of $\hat{Bias}\left(\hat{\mu}_{F,naive}^{2002}\right)$, were calculated using Eq. (5). Finally, two estimates, $\hat{\mu}_F^{2002}$, from Eq. (6) and two variance estimates, $\hat{Var}(\hat{\mu}_F^{2002})$, from Eq. (7) were then calculated. The same procedure was used to obtain the comparable 2007 estimates, $\hat{\mu}_{F,naive}^{2007}$, $\hat{Bias}\left(\hat{\mu}_{F,naive}^{2007}\right)$, $\hat{\mu}_F^{2007}$, and $\hat{Var}(\hat{\mu}_F^{2007})$. For each image date, only one naïve estimate could be calculated, but because there were two accuracy assessment datasets for each image date, two estimates of the other parameters were calculated.

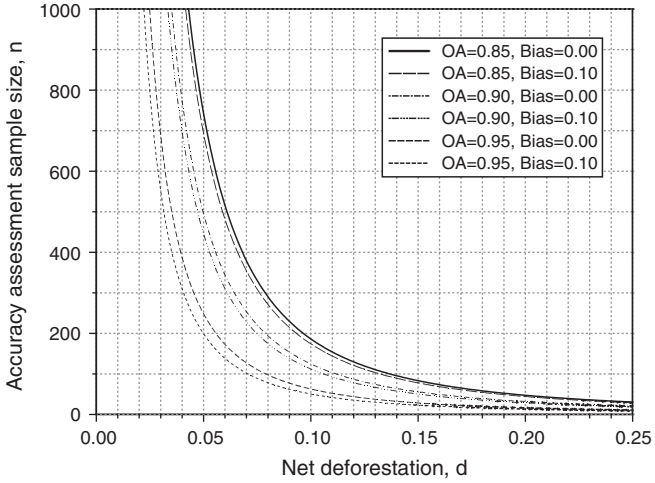

Fig. 2. Accuracy assessment sample size for significance level of $\alpha = 0.05$ and statistical power of $1\text{-}\beta = 0.80$.

Estimates of net deforestation, $\Delta\hat{\mu}_F = \hat{\mu}_F^{2007} - \hat{\mu}_F^{2002}$, using Eq. (9) and $\hat{Var}(\Delta\hat{\mu}_F)$ using Eqs. (10a) and (10b) were calculated separately for the combination of the $A_{2002\text{-}1}$ and $A_{2007\text{-}1}$ accuracy assessment datasets and for the combination of the $A_{2002\text{-}2}$ and $A_{2007\text{-}2}$ accuracy assessment datasets. Because the observations for the $A_{2002\text{-}1}$ and $A_{2007\text{-}1}$ datasets were independent, $\hat{Cov}(\hat{\mu}_F^{2002}, \hat{\mu}_F^{2007}) = 0$ so that Eq. (10b) could be used to calculate $\hat{Var}(\Delta\hat{\mu}_F)$. However, because the $A_{2002\text{-}2}$ and $A_{2007\text{-}2}$ datasets include measurements of the same plots, the variance estimate was calculated using Eq. (10a) with $\hat{Cov}(\hat{\mu}_F^{2002}, \hat{\mu}_F^{2007})$ calculated using Eq. (11). For the latter approach, classification errors for the same plots were expected to be positively correlated so that $\hat{Cov}(\hat{\mu}_F^{2002}, \hat{\mu}_F^{2007}) > 0$ which, in turn, meant that $\hat{Var}(\Delta\hat{\mu}_F)$ for the second approach could be less than for the first approach.

4. Results and discussion

4.1. Sample size determination

The relationship between accuracy assessment sample sizes, n, OA, and $Bias\left(\hat{\mu}_{F,naive}\right)$, for magnitudes of net deforestation, d, that can be detected as statistically significant at $\alpha = 0.05$ with statistical power, $1\text{-}\beta = 0.80$, is depicted in Fig. 2. The graphs indicate that large sample sizes, large OAs, or both, are necessary for estimates of even moderately small magnitudes of net deforestation to be detected as statistically significantly different from zero. Smaller values of 1-α and 1-β would yield smaller values of n, as would accuracy assessment datasets with correlated observations such as for $A_{2002\text{-}2}$ and $A_{2007\text{-}2}$. These sample size estimates are based on an assumption of simple random sampling. Cluster sampling, which is often used for forest inventories, would yield different sample size estimates, depending on factors such as the number of clusters, the number of plots per cluster, and the correlation among observations of plots for the same cluster.

4.2. Accuracy assessment

Assessment of the quality of fit of the logistic regression model to the forest/non-forest observations indicated no serious concerns regarding lack of model fit.

Estimates of accuracy measures for the forest/non-forest classifications obtained from the error matrices (Table 2) varied: PAs for non-forest ranged approximately from 0.78 to 0.83 and for forest approximately from 0.86 to 0.93; UAs for non-forest ranged approximately from 0.73 to 0.84 and for forest approximately from 0.90 to 0.92; and OAs ranged approximately from 0.85 to 0.88. The OAs are similar, although slightly smaller, than those reported for other studies in this region (Finley et al., 2008; Haapanen et al., 2004; McRoberts, 2006) and for other studies using the logistic regression model (Fraser & Latifovic, 2005; Fraser et al., 2003, 2005; Wulder et al., 2006).

Table 2
Error matrix for 2002 classification using $A_{2002\text{-}2}$ accuracy assessment dataset.

		Predicted class		Total	Producer's Accuracy (PA)
		$\frac{0}{(NF)}$	$\frac{1}{(F)}$		
Observed class	0 (NF)	50	10	60	0.8333
	1 (F)	18	117	135	0.8667
Total		68	127	195	
User's accuracy (UA)		0.7353	0.9213		OA=0.8564

Several approaches may be considered for increasing OAs. First, more accurate GPS receivers would increase the probability that ground plots are associated with correct pixels. Misregistration of plots and imagery is known to have serious detrimental consequences for land cover classifications, particularly for land cover change classifications (Dai & Khorram, 1998; Magnussen, 2007). McRoberts (2010) demonstrated that location errors characteristic of the GPS receivers used by FIA field crews may result in nearly half of FIA plots being associated with incorrect Landsat pixels. Second, greater comparability between the ground plot and pixel sizes would contribute to enhancing the model relationship by increasing the probability that the plots adequately characterize entire pixels. Finally, a model form that better characterizes the relationship between the plot observations and the pixel spectral transformations would contribute to fewer misclassifications.

4.3. Estimates of proportion forest

Naïve estimates of proportion forest for the entire study area were $\hat{\mu}_{F,naive}^{2002} = 0.5937$ and $\hat{\mu}_{F,naive}^{2007} = 0.6435$ with bias estimates in the range $-0.0321 \leq \hat{Bias}(\hat{\mu}_F) \leq 0.0206$ (Table 3). Estimates of proportion forest obtained for the model-assisted estimator were $\hat{\mu}_F^{2002-1} = 0.6258$, $\hat{\mu}_F^{2002-2} = 0.6347$, $\hat{\mu}_F^{2007-1} = 0.6229$, and $\hat{\mu}_F^{2007-2} = 0.6230$ with standard errors in the range $0.0241 \leq SE(\hat{\mu}_F) \leq 0.0284$. Coefficients of variation for estimates of proportion forest were in the range $0.0387 \leq \frac{SE(\hat{\mu}_F)}{\hat{\mu}_F} \leq 0.0454$ with slightly smaller values for the 2007 classification.

When estimating proportion forest using the simple random sampling (SRS) estimators, observations for all 249 plots measured in both 2002 and 2007 were used because issues related to whether forest/non-forest observations for the smaller plots adequately represent the larger pixels are irrelevant. Plots with forest land use observations but with no volume were considered to have non-forest cover. The resulting confidence intervals in the form, $\hat{\mu}_F \pm t_{1-\alpha/2}\sqrt{\hat{Var}(\hat{\mu}_F)}$, were 0.5963 ± 0.0620 for 2002 and 0.5816 ± 0.0624 for 2007.

4.4. Estimates of net deforestation

Confidence intervals for estimates of net deforestation for the entire study area, calculated as $\Delta\hat{\mu}_F \pm t_{1-\alpha/2}\sqrt{\hat{Var}(\Delta\hat{\mu}_F)}$, were -0.0029 ± 0.0746 for the $A_{2002\text{-}1}$ and $A_{2007\text{-}1}$ accuracy assessment datasets with independent observations and -0.0117 ± 0.0456 for the $A_{2002\text{-}2}$ and $A_{2007\text{-}2}$ accuracy assessment datasets with positively

Table 3
Estimates for proportion forest.

Date	Plot-based estimates			Remote sensing-based estimates						
	n	$\hat{\mu}_F$	$SE(\hat{\mu}_F)$	Training dataset	$\hat{\mu}_{F,naive}$	Accuracy assessment dataset	n	$\hat{Bias}\left(\hat{\mu}_{F,naive}\right)$	$\hat{\mu}_F$	$SE(\hat{\mu}_F)$
2002	249	0.5963	0.0310	T_{2002}	0.5937	$T_{2002\text{-}1}$	187	−0.0321	0.6258	0.0284
						$T_{2002\text{-}2}$	195	−0.0410	0.6347	0.0272
2007	249	0.5816	0.0312	T_{2007}	0.6435	$T_{2007\text{-}1}$	194	0.0206	0.6229	0.0242
						$T_{2007\text{-}2}$	195	0.0205	0.6230	0.0241

correlated observations. The confidence interval for net deforestation obtained using the SRS estimators and observations for all 249 plots was -0.0148 ± 0.0362. Although the SRS standard errors for estimates of proportion forest for individual years were larger than the corresponding model-assisted standard errors, the SRS standard error for the estimate of net deforestation was smaller than the model-assisted estimates. This result partially reflects the larger correlation, $\hat{Cov}(\hat{\mu}_F^{2002}, \hat{\mu}_F^{2007}) \approx 0.0008$, between estimates of proportion forest for the two years using the SRS estimators than $\hat{Cov}(\hat{\mu}_F^{2002}, \hat{\mu}_F^{2007}) = 0$ which was assumed when using the model-assisted estimators with the $A_{2002\text{-}1}$ and $A_{2007\text{-}1}$ accuracy assessment datasets, and $\hat{Cov}(\hat{\mu}_F^{2002}, \hat{\mu}_F^{2007}) \approx 0.0004$ calculated for the $A_{2002\text{-}2}$ and $A_{2007\text{-}2}$ accuracy assessment datasets.

The plot-based SRS estimate and the two remote sensing, model-assisted estimates of net deforestation were negative, meaning a net loss of forest cover between the 2002 and 2007, although none of the three estimates was statistically significantly different from zero. Further, apart from correlation between the plot-based and remote sensing-based estimates as a result of using the same data which was ignored, no estimate was statistically significantly different from either of the other two estimates.

An important potential advantage of the model-assisted estimators is that the relationship between the remotely sensed data and the ground plot data can be exploited to obtain smaller standard errors of estimates. Although this potential was realized for estimates of proportion forest, it was not realized for estimates of net deforestation. Failure to realize the potential can be attributed to multiple factors. First, the larger estimated covariance between the SRS estimates of proportion forest for the two years than the model-assisted covariance estimates contributed to a smaller SRS standard error as calculated using Eqs. (10a) and (10b). Second, less severe data filtering as described in Section 4.2 would have increased the accuracy assessment sample sizes, reduced the model-assisted standard error estimates, and contributed to greater precision for the model-assisted estimates of net deforestation. Third, larger OAs would also have reduced the model-assisted standard errors.

The effects of sample sizes and classification accuracies on estimates of net deforestation merit considerable attention. First, when the proportion of plots whose land cover changes from forest to non-forest is small, possibilities for direct classification of forest change and assessment of accuracy for a change classification obtained from independent forest/non-forest classifications are extremely limited. A potential solution to this difficulty is to use a stratified sampling design with strata based on expected change classes obtained from a preliminary change map, knowledge of transportation networks, or proximity to population centers. However, because ground sampling is expensive, the current tendency is to use existing data rather than initiate a second, independent sampling effort. Second, the utility of the model-assisted approach to produce more precise estimates of net deforestation than estimates based on plot data only requires large OAs resulting from strong relationships between forest/non-forest observations and remote sensing-based auxiliary variables. For small estimates of net deforestation to be detected as statistically significantly different from zero, large accuracy assessment sample sizes may be required, even with large OAs (Walsh & Burk, 1993).

Finally, an advantage of the remote sensing-based approach is that a map depicting classes of forest change may be obtained as a by-product, although the utility of the map may be influenced by estimates of accuracy and bias (Fig. 3).

5. Conclusions

Three conclusions may be drawn from the study. First, a probability-based (design-based), post-classification approach to formulating inferences in the form of confidence intervals for remote sensing-based estimates of net deforestation using the model-assisted estimator has been derived and illustrated. Although the particular classification procedure used for illustrative purposes was based on the logistic regression model, the approach to inference

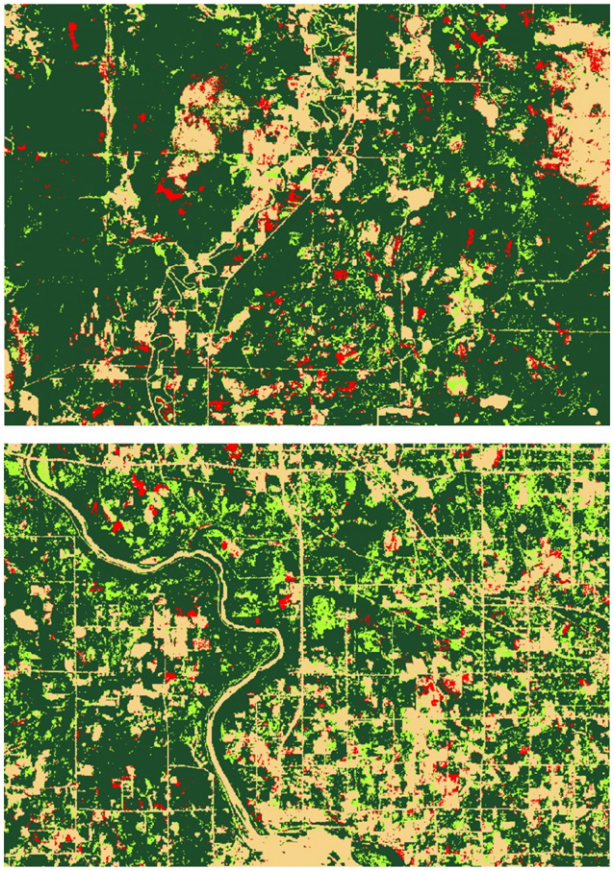

Fig. 3. Change maps for approximately 19.4-km × 13.5-km areas: dark green: F-F; tan: NF-NF; bright green: NF-F; red: F-NF.

may be used with multiple classification procedures. Second, remote sensing-based estimates of net deforestation were small, less in absolute value than 0.015, and were not statistically significantly different from zero. Third, the relatively large accuracies and accuracy assessment sample sizes necessary for meaningful magnitudes of net deforestation to be detected as statistically significant cannot be ignored. This conclusion is particularly relevant for tropical deforestation studies for which accuracies may be small due to the lack of good training data and accuracy assessment sample sizes may be small due to logistical and financial constraints, particularly when forest lands are remote and inaccessible.

References

Achard, F., Eva, H. D., Stibig, H. -J., Mayaux, P., Gallego, J., Richards, T., et al. (2002). Determination of deforestation rates of the world's humid tropical forest. *Science*, *297*, 999–1002.

Agresti, A. (2007). *An introduction to categorical data analysis.* Hoboken, NJ: Wiley-Interscience.

Card, D. H. (1982). Using known map category marginal frequencies to improve estimates of thematic accuracy. *Photogrammetric Engineering and Remote Sensing*, *48*, 431–439.

Congalton, R. G. (1991). A review of assessing the accuracy of classifications of remotely sensed data. *Remote Sensing of Environment*, *37*, 35–46.

Coppin, P., Jonckheere, I., Nackaerts, K., & Muys, B. (2004). Digital change detection methods in ecosystem monitoring: A review. *International Journal of Remote Sensing*, *25*(9), 1565–1596.

Crist, E. P., & Cicone, R. C. (1984). Application of the tasseled cap concept to simulated Thematic Mapper data. *Photogrammetric Engineering and Remote Sensing*, *50*, 343–352.

Czaplewski, R. L., & Catts, G. P. (1992). Calibration of remotely sensed proportion or areal estimates for misclassification error. *Remote Sensing of Environment*, *39*(1), 29–43.

Dai, X., & Khorram, S. (1998). The effects of image misregistration on the accuracy of remotely sensed change detection. *IEEE Transactions on Geoscience and Remote Sensing*, *36*(5), 1566–1577.

Dinerstein, E., Olson, D. M., Graham, D. J., Webster, A. V., Primm, S. A., Bookbinder, M. P., et al. (1995). *Una evaluación del estado de conservación de las ecoregiones terrestres de América Latina y el Caribe.* Banco Mundial, Washington, D.C: Publicado en colaboración con el Fondo Mundial para la Naturaleza.

Finley, A. O., Banerjee, S., & McRoberts, R. E. (2008). A Bayesian approach to multi-source forest area estimation. *Environmental and Ecological Statistics*, *15*(2), 241–258.

Food and Agriculture Organization of the United Nations (FAO) (2005). Global resources assessment 2005. *Progress towards sustainable forest management. FAO forestry Paper 147* Rome. 323 p. Available at: http://www.fao.org/docrep/008/a0400e/a0400e00.htm. (last accessed: May 2008).

Fraser, R. H., Abuelgasim, A., & Latifovic, R. (2005). A method for detecting large-scale forest cover change using coarse spatial resolution imagery. *Remote Sensing of Environment*, *95*, 414–427.

Fraser, R. H., Fernandes, R., & Latifovic, R. (2003). Multi-temporal mapping of burned forest over Canada using satellite-based change metrics. *Geocarto International*, *18*(2), 37–47.

Fraser, R. H., & Latifovic, R. (2005). Mapping insect-induced defoliation and mortality using coarse spatial resolution satellite imagery. *International Journal of Remote Sensing*, *10*(1), 193–200.

Giardin, C. (2010). *UN-REDD/FAO to publish national forest MRV system recommendations.* UN-REDD Programme Newsletter Issue 8, May 2010. Available at: http://www.un-redd.org/Newsletter8_MRV_System_Recommendations/tabid/4551/language/en-US/Default.aspx. Last accessed: June 2011.

Global Forest Watch (GFW) (2006). Frequently asked questions. http://www.globalforestwatch/english/about/faqs.htm (last accessed 08 January 2007).

GOFC-GOLD (2010). A sourcebook of methods and procedures for monitoring and reporting anthropogenic greenhouse gas emissions and removals caused by deforestation, gains and losses of carbon stocks in forests remaining forests and forestation. *GOFC-GOLD Report version COP16-1.* Alberta, Canada: GOFC-GOLD Project Office, Natural Resources Canada Available at: http://www.gofc-gold.uni-jnea.de/redd/

Groombridge, B., & Jenkins, M. D. (2002). World atlas of biodiversity. Berkeley: University of California Press (340 pp.).

Gullison, R. E., Frumhoff, P. C., Canadel, J. G., Field, C. G., Nepstad, D. C., Hayhoe, K., et al. (2007). Tropical forests and climate policy. *Science*, *316*, 985–986.

Haapanen, R., Ek, A. R., Bauer, M. E., & Finley, A. O. (2004). Delineation of forest/nonforest land use classes using nearest neighbor methods. *Remote Sensing of Environment*, *89*(3), 265–271.

Hansen, M. H., Madow, W. G., & Tepping, B. J. (1983). An evaluation of model-depending and probability-sampling inferences in sample surveys. *Journal of the American Statistical Association*, *78*, 776–793.

Hayes, C. J., & Cohen, W. B. (2007). Spatial, spectral, and temporal patterns of tropical forest cover change as observed with multiple scales of optical satellite imagery. *Remote Sensing of Environment*, *106*, 1–16.

Hayes, D. J., & Sader, S. A. (2001). Comparison of change-detection techniques for monitoring tropical forest clearing and vegetation regrowth in a time series. *Photogrammetric Engineering and Remote Sensing*, *67*(9), 1067–1075.

Holdridge, L. R. (1947). Determination of world plant formation from simple colmatic data. *Science*, *105*, 367–368.

Holdridge, L. R. (1967). *Life zone ecology.* San Jose, CA: Tropical Science Center.

Hosmer, D. W., & Lemeshow, S. (1989). *Applied logistic regression.* New York: John Wiley & Sons, Inc.

Kauppi, P. E., Ausubel, J. H., Fang, J., Mather, A. S., Sedjo, R. A., & Waggoner, P. E. (2006). Returning forests analyzed with the forest identity. *Proceedings of the National Academy of Sciences*, *103*(46), 17574–17579.

Kauth, R. J., & Thomas, G. S. (1976). The Tasseled Cap — A graphic description of the spectral–temporal development of agricultural crops as seen by Landsat. *Proceedings of the symposium on machine processing of remotely sensed data* (pp. 41–51). West Lafayette, IN: Purdue University.

Kennedy, R. E., Cohen, W. B., & Schroeder, T. A. (2007). Trajectory-based change detection for automated characterization of forest disturbance dynamics. *Remote Sensing of Environment*, *110*, 370–386.

Kennedy, R. E., Townsend, P. A., Gross, J. E., Cohen, W. B., Bolstad, P., Wang, Y. Q., et al. (2009). Remote sensing change detection tools for natural resource managers: Understanding concepts and tradeoffs in design of landscape monitoring projects. *Remote Sensing of Environment*, *113*, 1382–1396.

Köhl, M., Baldauf, T., Plugge, D., & Krug, J. (2009). Reduced emission from deforestation and forest degradation (REDD): A climate change mitigation strategy on a critical track. *Carbon Balance and Management*, *4*(10) (Open source).

Magnussen, S. (2007). A method for estimation of a land-cover change matrix from error-prone unit-level observations. *Canadian Journal of Forest Research*, *37*, 1505–1517.

Mas, J. -F. (1999). Monitoring land-cover changes: A comparison of change detection techniques. *International Journal of Remote Sensing*, *20*(1), 139–152.

Matthews, E., Payne, R., Rohwede, M., & Siobahn, M. (2000). *Pilot analysis of global ecosystems: Forest ecosystems.* Washington, DC: World Resources Institute 86 pp.

McRoberts, R. E. (2006). A model-based approach to estimating forest area. *Remote Sensing of Environment*, *103*, 56–66.

McRoberts, R. E. (2010). The effects of rectification and Global Positioning System errors on satellite image-based estimates of forest area. *Remote Sensing of Environment*, *114*, 1710–1717.

McRoberts, R. E., Bechtold, W. A., Patterson, P. L., Scott, C. T., & Reams, G. A. (2005). The enhanced Forest Inventory and Analysis program of the USDA Forest Service: Historical perspective and announcement of statistical documentation. *Journal of Forestry*, *103*(6), 304–308.

Meyfroidt, P., Rudel, T. K., & Lambin, E. F. (2010). Forest transitions, trade, and the global displacement of land use. *Proceedings of the National Academy of Sciences*, *107*(49), 20917–20922.

Muchoney, D. M., & Haack, B. N. (1994). Change detection for monitoring forest defoliation. *Photogrammetric Engineering and Remote Sensing*, *60*(10), 1243–1251.

Nabuurs, G. J., & Masera, O. (2007). Forestry. Chapter 9. In B. Metz, O. R. Davidson, P. R. Bosch, & L. A. Meyer (Eds.), *Climate change 2007: Mitigation of climate change. Contribution of working group III to the fourth assessment report of the intergovernmental panel on climate change* Available at: http://www.ipcc.ch/publications_and_data/publications_ipcc_fourth_assessment_report_wg3_report_mitigation_of_climate_change.htm. Last accessed: June 2011.

Rouse, J. W., Haas, R. H., Schell, J. A., & Deering, D. W. (1973). Monitoring vegetation systems in the great plains with ERTS. *Proceedings of the Third ERTS Symposium. NASA SP-351, Vol. 1.* (pp. 309–317) Washington, DC: NASA.

Särndal, C. -E., Swensson, B., & Wretman, J. (1992). *Model assisted survey sampling.* New York: Springer 693 pp.

Singh, A. (1989). Digital change detection techniques using remotely-sensed data. *International Journal of Remote Sensing*, *10*(6), 989–1003.

Van Deusen, P. C. (1994). Correcting bias in change estimates from thematic maps. *Remote Sensing of Environment*, *50*, 67–73.

Walsh, T. A., & Burk, T. E. (1993). Calibration of satellite classifications of land area. *Remote Sensing of Environment*, *46*, 281–290.

Watson, C. (2009). *Forest carbon accounting: Overview and principles.* 39 pp. United Nations Development Program and United Nations Environment Program Available at: http://www.undp.org/climatechange/carbon-finance/Docs. Last accessed: June 2011.

Wulder, M. A., White, J. C., Bentz, B., Alvarez, M. F., & Coops, N. C. (2006). Estimating the probability of mountain pine beetle red-attack damage. *Remote Sensing of Environment*, *101*, 150–166.